17

Planar Antennas For Satellite Communications

Jorge Sosa-Pedroza, Fabiola Martínez-Zúniga and Mauro Enciso-Aguilar
Instituto Politécnico Nacional. Escuela Superior de Ingeniería Mecánica y Eléctrica
México

1. Introduction

Modern Satellite Communications requires the development of very small size, low-cost, low-profile, high gain and high directivity antennas. Antennas form the link between transmitting and receiving equipment and the space propagation path. Even the general principles may apply to satellite communications antennas, imposed limitations of gain, field pattern and mainly the physical environment lead to design requirements which should be taken in account. Most satellite antennas are designed to give coverage over a specified restricted area defining restrictions over antenna gain; on the other hand payload restrictions of weight and size lead to small size and weight antennas. Especially for these characteristics, planar antennas could have wide application on communications satellites. Since the late 1970s, the international antenna community has devoted much effort to the theoretical and experimental research on microstrip and printed antennas, which offer the advantages of low profile, compatibility with integrated circuit technology and conformability to a shaped surface. The results of this research have contributed to the success of these antennas not only in military applications such as aircraft, missiles, and rockets but also in commercial areas such as mobile satellite communications, the Direct Broadcast Satellite (DBS) system, global position system (GPS) and remote sensing but their main applications are on ground transceivers. Last two decades have been especially worthwhile on planar antennas development, mainly for mobile communications, but its applications should be extended to satellite systems. Particularly for the first Mexican satellite system (Morelos I and II), primary array receiving Ku band , was a planar array to produce an elliptical footprint over Mexican territory. For the second generation of Mexican satellites, was introduced the L band circular polarization array, formed by 16 parabolic reflectors feed by crossed short dipoles producing the needed circular polarization and also an elliptical footprint. It is clear that if there were used a planar array, as those that technology has developed in the last two decades, the cost and the weight would be reduced to a fourth part. This chapter of the Satellite Communications book, is devoted to planar antennas, not only for that already in use but proposing other kind that could be applied for satellite communications. It starts with a brief description of planar antennas, their characteristics, and their applications as antenna arrays. The next part will describe actual planar antennas used in satellite communications systems and will finish with a proposal of new developments of planar antennas that could be used in the near future.

1.1 A Brief History

Historically microstrip antennas and consequently planar antennas, have associated with low cost and low profile, but this simplistic description is inadequate as state in (James et al.,

1989), considering that the feasibility of a low profile printed radiator has inspired the system creator with abundance of examples, as the printed paper antennas, or adaptive conformal antenna arrays and many other examples. The success on cellular telephony is based in much in the planar antenna development, as the services offered by cellular company's increase every day, planar ultra wideband antennas are an actual challenge for those working in the area. Research and engineering publications are also devoting more space to development in planar antennas; one can open any proceedings on antennas and will find at least one or two articles related with this subject. Satellite communications are not outside of this boom, especially when, as in no other industry, low weight, low profile and low cost are a daily challenge for antenna design. The invention of the microstrip concept has been attributed to many sources and the earliest include (Greig et al., 1952), and Deschamps (1953), the idea was to create a new way for connecting electronic circuits even knowing the high unwanted radiation, leading to reduce both, substrate and conducting strip. Whether the advent of the transistor influenced the rapid development of printed circuits, the main interest was the development of low cost microwave circuits (James et al., 1981). There were few proposals to use the technique for antennas in those early years, until the 1970's when the new generation of missiles create the need of low profile antennas, after that the development of microstrip and planar antennas started to fill up research publications. A key point on the design of microstrip and planar antennas, was the development of substrates, not only to define characteristics of permittivity and low loss tangent but also to make materials capable to work on extreme ambient conditions; the 80's was the decade when bigger steps were done in substrate design, however as the frequency demand increases in communication systems, the development of new materials has lead to manufacturers in tightened their specifications, and reducing substrate costs. Table 1 shows examples of materials actually used in microstrip and planar antennas.

Type	Composition	Thickness	ϵ_r	$\tan\delta$
RO3010	PTFE Ceramic	0.005"-0.050"	10.2±0.30	0.0023
RO3206	PTFE Woven Glass	0.005"-0.050"	6.15±0.15	0.0027
RO4350B	Hydrocarbon Ceramic	0.004"-0.06"	3.48±0.05	0.0037
RT/Duroid 5880	PTFE Glass Fiber	0.005"-0.125"	2.20±0.02	0.0009
RT/Duroid 6006	PTFE Ceramic	0.005"-0.100"	6.15±0.15	0.0027
TMM 3	Hydrocarbon Ceramic	0.15"-0.125"	3.27±0.032	0.0020
TMM 10	Hydrocarbon Ceramic	0.015"-0.100"	9.20±0.23	0.0022
FR-4	Woven Glass/Epoxy Resin	0.059"-0.118"	4.8 and 2.2	0.017

Table 1. Typical substrate materials for planar antennas

Planar antennas have influenced other fields in electromagnetics, those related with materials and the development of transmission lines; actually engineers include the feeders as a part of the design of patch antennas to get a better control over the input impedance characteristics, this is even more important for large arrays architectures where the feeders and antennas are regarded as a complete entity, emphasizing the importance of choice of array topology and the fact that feeders cannot necessarily be freely attached to printed elements. On the other hand, analytical development of antennas is no longer applied; the actual printed substrate technology uses mathematical models as the Finite Difference on Time Domain (FDTD) (Yee, 1966) or the Method of Moments (Harrington, 1992) and others, managed by computer simulators, reducing the highly mathematical analysis to a drawing in a CAD system, which determines current distribution, and after that, radiation patterns, gain, feeder impedance and

other parameters of antennas and antenna arrays. Computational Electromagnetics is a field in constant development, seeking for better computer characteristics and computer architecture, as the parallel computer systems, as well for better programming efficiency.

2. Microstrip Antennas

Microstrip antennas are very attractive to be used as radiators in satellite communications systems because of its several interesting features like low profile, light weight, easy fabrication, robust nature, conformability to mounting hosts, compatibility with microwave monolithic integrated circuits (MMICs) and optoelectronic integrated circuits (OEICs) technologies, they are very versatile in terms of resonant frequency, polarization, radiation pattern and impedance Microstrip antennas were first introduced in the mid of 70s (Howell, 1975; Munson, 1974) since then a really intense research activity on microstrip antenna has been taken place around the world for both academic and industrial entities. The basic configuration of a microstrip patch antenna is shown in Fig. 1.

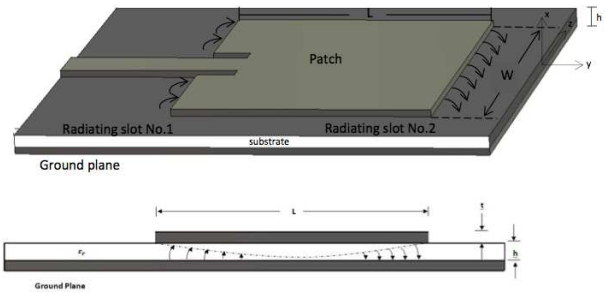

Fig. 1. Microstrip patch antenna configuration

It consist of a dielectric substrate sandwiched structure. The upper surface supports a printed conducting radiator strip or *patch* (even if a microstrip antenna is essentially different to a *patch* antenna, we will use both terms indifferently in this subsection) which is well contoured while the entire lower surface of the substrate is backed by the ground plane. The microstrip patch is designed in a such way that its maximum radiation pattern is normal to the surface of the patch (broadside radiator). This can be achieved by choosing the mode of excitation beneath the patch (Balanis, 2005). The patch radiates from fringing fields around its edges. Impedance match occurs when a patch resonates as a resonant cavity. When matched, the antenna achieves peak efficiency. For microwave applications, thinner substrates with higher dielectric constants are desirable because they require tightly bound field to decrease parasitics effects like undesired radiation and coupling. This also leads to smaller element sizes.
The shape of the patch can take several geometrical forms like square, rectangular, circular, triangular, elliptical, linear (thin strip dipole) or any other configuration. The most common patch shapes are square, rectangular, and circular due to its simplicity of design, manufacture and analysis. They are also attractive because of their radiation characteristics, especially for low cross-polarization radiation. Linear and circular polarization can be obtained by either one element or an array of microstrip antennas. Rectangular patches tend to have the largest impedance bandwidth, simply because they are larger than the other shapes. Circular and elliptical patches are slightly smaller than their rectangular counterpart and as a result have

slightly lower gain and bandwidth. One of the primary reasons the circular geometry was intensively investigated in the past was because of its symmetry allowed full-wave analysis tools utilizing a spectral domain technique. Circular patch antennas provide circularly polarized conical patterns for effective data transmission from a satellite to the earth at UHF and S-band frequencies. In the following sections we shall briefly introduce the theoretical framework of only two types of patch: rectangular and circular. Full wave methods like Method of Moments and FDTD along computational tools are discussed later in this chapter.

3. Main Figures of Merit of Microstrip Antennas

3.1 Resonant Frequency

In general, microstrip antennas are half-wavelength structures and are operated at the fundamental resonant mode TM_{01} or TM_{10}, with a resonant frequency given by (James et al., 1989):

$$f_r = \frac{c}{2L\sqrt{\epsilon_r}} \tag{1}$$

The above expression is only valid for a rectangular microstrip antenna with a thin microwave substrate, where c is the speed of light, L is the patch length of the rectangular microstrip antenna, and ϵ_r is the relative permittivity of the grounded microwave substrate. From 1 it is clear that the microstrip antenna has a resonant length inversely proportional to $\sqrt{\epsilon_r}$, hence the use of a microwave substrate with a larger permittivity thus can result in a smaller physical antenna length at a fixed operating frequency.

If the open-end extension due to fringing effect is considered then the resonant frequency for a rectangular microstrip antenna becomes (Hirazawa et al., 1992; James et al., 1989):

$$f_r \cong \frac{c}{2L_{eff}\sqrt{\epsilon}_{eff}} \tag{2}$$

where:

$$L_{eff} = L\left\{1 + 0.824\frac{h}{L}\frac{(\epsilon_{eff} + 0.3)(L/h + 0.262)}{(\epsilon_{eff} - 0.258)(L/h + 0.813)}\right\} \tag{3}$$

$$\epsilon_{eff} = \frac{\epsilon_r + 1}{2} + \frac{\epsilon_r - 1}{2}\left(1 + 10\frac{L}{h}\right)^{-\frac{1}{2}} \tag{4}$$

with h being the substrate thickness. If the microstrip antenna is circular then its resonant frequency is approximated by:

$$f_r \cong \frac{\chi_{11}c}{2a_{eff}\sqrt{\epsilon}_r} \tag{5}$$

where

$$a_{eff} = L\left\{1 + \frac{2h}{\pi a\epsilon_r}\ln\frac{\pi a}{2h} + 1.7726\right\}^{\frac{1}{2}} \tag{6}$$

and

$$\chi_{11} = 1.841 \tag{7}$$

a being the radius of the patch.

3.2 Radiation Pattern

It is quite hard to talk on radiation pattern characteristics without associate it with the internal construction consideration. Here we only briefly discuss the associated internal structures that affect the pattern. Rectangular and circular are the most common shapes for patch and they radiate similar patterns. When the cavity is loaded in order to shrink its size, it radiates wider beamwidth patterns that decreases directivity. Structures that couple to coplanar patches to increase the impedance bandwidth will radiate narrower beams, but the basic patch has a wide beamwidth. If multiple coplanar patches are coupled, one can expect the pattern to narrow or vary its shape as the mixture of modes on the various patches changes over the frequency range of operation(Milligan, 2005). Radiation pattern of microstrip antennas have been investigated by several techniques including the equivalent magnetic current method (Derneryd, 1976; James et al., 1989; Long, 1978), full-wave analysis (Chang, 1989; Itoh et al., 1981), and method of moments (Agrawal et al., 1977; Chang, 1989). The former has been often used because its procedural simplicity and extensive applicability. This method considers magnetic current sources $\mathbf{K}_{m1}$ and $\mathbf{K}_{m2}$ laying at the edge or within the vicinity of the edge of the patch that can be approximated by a magnetic current loop antenna. The radiation pattern can be determined by using a Hertz or potential vector. Fig. 2 depicts the fringing electric fields around the edges of square and circular patch antennas excited in the lowest-order cavity modes. The arrow sizes indicate the magnitude of the fields. As seen the square patch exhibit nearly uniform fields along two edges called the width, and a sinusoidal evolution along the other two edges, called the resonant length. The fields vanish along a virtual electrically short-circuited plane halfway across the patches. On either side of the short-circuit plane, the fields are directed in opposite directions.

The circular patch fringing fields distribution varies as $\cos\phi$, where the angle ϕ along the edge is measured from the peak electric field. Magnetic currents found from the fringing electric fields can replace the electric currents located on the patch and the surrounding ground plane for pattern analysis.

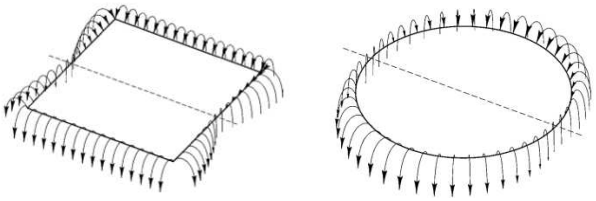

(a) Square (b) Circular

Fig. 2. Fringing electric fields around microstrip patches: (a) square; (b) circular.(After (Milligan, 2005))

The source of equivalent magnetic current corresponding to the E_z field component (along the vertical direction) of a dominant mode is expressed taking the image component as $\mathbf{K}_m = 2\mathbf{E}_z \times \mathbf{n}$, $\mathbf{n}$ being a unity normal vector. The pattern is determined by the line integration of $\mathbf{K}_m$ at the rim of the patch over the adjacent source region (James et al., 1989). For a circular patch with a TM_{110} dominant mode, the expressions to approximate the pattern are: (Hirazawa et al., 1992; James et al., 1989; Long, 1978):

$$E_\theta = -jK_d a\cos(\phi)\sin(m)\left\{\frac{J_1'(n)}{\cos\theta}\right\} \tag{8}$$

$$E_\phi = \frac{jK_d}{k_0}\sin(\phi)\cos(m)\left\{\frac{J_1(n)}{\cos\theta}\right\} \tag{9}$$

with

$$m = k_0 h\cos\theta;\;\; n = k_0 a\sin\theta;\;\; K_d = E_0\frac{e^{-jk_0R}}{R}J_1(ka) \tag{10}$$

For a rectangular patch with a dominant TM_{100} mode the expression for the radiation pattern are given by:

$$E_\theta = -jK_r f(\theta,\phi)\cos\phi\left\{\frac{\epsilon_r - \sin^2\theta}{\epsilon_r - (\sin\theta\cos\phi)^2}\right\} \tag{11}$$

$$E_\phi = jK_r f(\theta,\phi)\cos\theta\sin\phi\left\{\frac{\epsilon_r}{\epsilon_r - (\sin\theta\cos\phi)^2}\right\} \tag{12}$$

with:

$$f(\theta,\phi) = \left\{\frac{\sin(m)}{m}\right\}\cos n;\; m = \frac{k_0 L}{2}\sin\theta\sin\phi;\; n = \frac{k_0 L}{2}\sin\theta\cos\phi;$$
$$K_r = \frac{V_0 k_0 L}{\pi}\frac{e^{-jk_0R}}{R};\; V_0 = E_0 h \tag{13}$$

where k_0 is the wave number in free space, k is the wave number in the substrate, $J(n)$, $J'(n)$ first kind of Bessel function and its derivative, respectively. E_0 is an arbitrary constant, h is the substrate thickness, a is the radio of the circular patch , L is the patch length of the rectangular shape.

3.3 Quality Factor, Radiation Efficiency, Bandwidth and Gain

The quality factor, bandwidth, and efficiency are antenna figures-of-merit, which are interrelated, and there is no complete freedom to independently optimize each one.The quality factor Q of a microstrip antenna becomes one of the most important design parameters. Quality Factor is a measure of the radiation loss in the microstrip antenna. For a given substrate characteristics like ϵ_r, tanδ, σ and a radiation pattern, the unloaded quality factor Q_0 and the radiation efficiency is (James et al., 1989; Long, 1978):

$$\frac{1}{Q_0} = \frac{1}{Q_r} + \frac{1}{Q_c} + \frac{1}{Q_d} \tag{14}$$

where

$$\eta = \frac{Q_0}{Q_r};\;\; Q_d = \frac{1}{tan\delta};\;\; Q_c = \frac{h}{\delta_s};\;\; \delta_s = \frac{1}{\sqrt{\pi f\mu_0\sigma}};\;\; Q_r = \omega\frac{W_T}{P_{rad}};\;\; W_T = \frac{1}{2}\epsilon\int_v |E|^2 dv \tag{15}$$

and

$$P_{rad} = \frac{1}{2}\Re\left\{\int_{sh}((E\times H)^*\cdot nds)\right\} = \frac{1}{2Z_0}\int_0^{2\pi}\int_0^{\frac{\pi}{2}}(|E_\theta|^2 + |E_\phi|^2)R^2\sin\theta d\theta d\phi \tag{16}$$

Q_r being the quality factor Q of radiation loss, δ_s skin depth, Q_c is Q of conductor loss, Q_d Q of dielectric loss, P_{rad} radiated power, P_{in} input power, Z_0 free space intrinsic impedance, $\Re$ real part, Sh sphere. Those expression agree well with measured values of Q_0 and η for common design ranges as long as the substrate is not thick enough to excite the surface wave and higher order modes (Hirazawa et al., 1992). In the general case the bandwidth of the antenna is expressed as:

$$BW = \frac{(VSWR - 1)}{Q_0\sqrt{VSWR}} \tag{17}$$

Then the BW of a practical antenna is determined for a given value of Q_0 and $VSWR$.

3.4 Directivity Gain

Directivity gain can be obtained by integrating the radiation pattern over an arbitrary surface containing the antenna. A useful expression to compute the directivity gain is:

$$G_d(\phi,\theta) = \frac{|E(\theta_0,\phi_0)|^2}{\frac{1}{4\pi}\int_0^{2\pi}\int_0^{\pi}|E(\theta,\phi)|^2\sin\theta d\theta d\phi} \tag{18}$$

where

$$|E(\theta,\phi)|^2 = |E_\theta(\theta,\phi)|^2 + |E_\phi(\theta,\phi)|^2 \tag{19}$$

and E_θ and E_ϕ are given by (8,), (9), (11,) and (12,)

3.5 Impedance Characteristics

Impedance characteristics of a microstrip antennas has been treated mainly from two points of view: self impedance and auto-impedance. Here the basic procedures for computing the impedance characteristics are briefly described.

3.5.1 Input Impedance

The Input impedance or self-impedance of a microstrip antennas has been studied by several models like Transmission Line Model (Derneryd, 1976; James et al., 1989) cavity model (Richards et al., 1979; 1981) and full wave models that includes several numerical techniques like method of moments (Gupta et al., 1988; Pozar, 1982) finite element (Volakis et al., 1998) and finite difference time domain method (FDTD) (Reineix et al., 1989; Sheen et al., 1990) among others. Transmission Line Model has been widely used because of its simplicity to describe the impedance of a general microstrip and provides a good physical insight, however it may lack in accuracy. In contrast, the cavity model is more accurate but at the same time, more complex although it also provides a good physical insight. Full wave models are in general very accurate and versatile and can manage a wide number of elements, complex patch shapes and coupling problems, but they are more complex models with less physical insight. Here we shall discuss the transmission line model only. In general, input impedance is complex and includes both a resonant an nonresonant components which is commonly reactive. Both real and imaginary parts of impedance vary with frequency. Ideally the reactance and the resistance exhibit symmetry about resonant frequency. At resonance, the reactance is equal to the average of the addition of its maximum and minimum values.

3.5.2 Transmission Line Model

The simplest analytical description of a rectangular microstrip patch utilizes transmission-line theory and models the patch as two parallel radiating slots (Munson, 1974). Each radiating edge of length L (Fig. 3) is modeled as a narrow slot radiating into a half-space,with a slot admittance given by (Harrington, 1961)

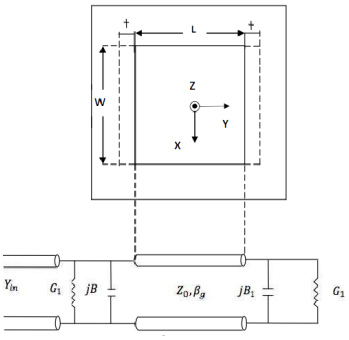

Fig. 3. Top view of a rectangular patch antenna and its associated transmission line equivalent circuit

$$G_1 + jB_1 \cong \frac{\pi q}{\lambda_0 \eta_0}[1 + j(1 - 0.636 \ln k_0 w)] \tag{20}$$

where λ_0 is the free-space wavelength, η_0 the intrinsic impedance of the free-space, $k_0 = \frac{2\pi}{\lambda_0}$ and w is the slot width, approximately equal to the substrate thickness h. Assuming that the field remains constant along the direction parallel to the radiating edge, the characteristic impedance is given by:

$$Z_0 = \frac{1}{Y_0} = \frac{t\eta_0}{L\sqrt{\epsilon_r}} \tag{21}$$

and the propagation constant is approximated by :

$$\beta_p \cong k_f \sqrt{\epsilon}_{eff} \tag{22}$$

where k_f is the propagation constant in free space. ϵ_{eff} is the effective dielectric constant given by:

$$\epsilon_{eff} = \frac{\epsilon_r + 1}{2} + \frac{\epsilon_r - 1}{2}\left(1 + 12\frac{h}{L}\right)^{-\frac{1}{2}} \tag{23}$$

The conductive component G_1 and the reactive component B_1 in (20) are related to the fringing effect and the radiation loss, and are approximated respectively by:

$$B_1 = \frac{k_f \Delta l}{Z_0}\sqrt{\epsilon_{eff}} \tag{24}$$

$$G_1 \approx \begin{cases} \frac{L^2}{90\lambda_0^2}, & L < 0.35\lambda_0 \\ \frac{L}{120\lambda_0} - \frac{1}{60\pi^2}, & 0.35\lambda_0 \leq L \leq 2\lambda_0 \\ \frac{L}{120\lambda_0}, & 2\lambda_0 < L \end{cases} \tag{25}$$

where Δl denotes the line extension due to fringing effect. This value can be expressed by:

$$\Delta l \approx 0.412t \frac{(\epsilon_{eff} + 0.3)}{(L/h + 0.264)} \tag{26}$$

The input admittance of the patch antenna on Fig. 3 can be treated as two slot antennas interconnected by a transmission line having characteristic admittance and propagation constant approximated by (20) and (22):

$$Y_{in} = G_1 + jB_1 + Y_0 \frac{(G_1 + jB_1) + jY_0 \tan(\beta_p L)}{Y_0 + j(G_1 + jB_1) \tan(\beta_p L)} \tag{27}$$

When the average stored magnetic and electric energies are equal then resonance occurs (Pozar, 2005), under these conditions the imaginary part of the admittance must vanish.

$$\Im \{Y_{in}\} = 0 \tag{28}$$

leading to:

$$\tan(\beta_p L) = \frac{2Y_0 B_1}{G_1^2 + B^2 - Y_0} \tag{29}$$

This condition is used to determine the resonant frequency for a given patch length L or inversely to establish the resonant leght L for a given resonant frequency. The input admittance at resonance is:

$$Y_{in} = 2G_1 \tag{30}$$

3.6 Arrays and feed networks

Even that most of the planar antennas are low and medium gain, wide pattern antennas, its versatility and mainly its low profile make them very popular in arrays. Its use to synthesize a required pattern is a nowadays application in many communication systems; most of the microstrip arrays are designed for fixed-beam broadside applications, increasing directivity and performing other functions, as for scanning purposes; those functions are difficult to obtain with a single radiator or even other classes of antennas; often the feed network is located coplanar with the array elements. The main versatility of planar antenna arrays is that the feed network usually is part of the printed environment; the elements can be feed by a single line in a series-feed network, or by multiple lines as a corporate-feed network (Balanis, 2005), including both parallel feed and hybrid series/parallel feed. Series-feed arrays are usually built using photolithography for both the radiating elements and the feed network, reducing its application to fixed beams, linear or planar arrays with single or dual polarization. In this configuration multiple elements are arranged linearly and feed serially by a single transmission line, multiple linear arrays can then be fed either serially or parallel to form a two dimensional planar array (Lee, 1997). Series-feed line can be in-line feed when all radiators are arranged in the same line or out-of-line feed when elements are parallel each other. The series-feed array can be classified as resonant and traveling-wave. For the first kind, impedances at the transmission line junctions and the patch elements are not matched and elements are spaced multiple integers of one wavelength apart creating a broadside beam, with a very narrow resonant bandwidth, around 1% . For the traveling wave array type, transmission line and elements are matched, with spacing of one wavelength for broadside or less for off-broadside radiation. The traveling current wave over the feeding line moves almost without reflections reducing almost to zero the energy at the end of array which can be either

absorbed by a matching network or reflected back to be reradiated in phase. Corporate feed arrays, also called parallel feed arrays, are more versatile and the designer has more control of the phase and amplitude of each feeding element, making them ideal for scanning phased arrays, multibeam arrays, or shaped-beam arrays.

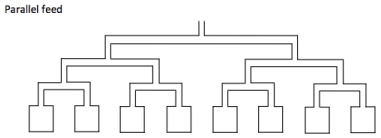

Fig. 4. Parallel feed configuration for microstrip arrays. After (Lee, 1997)

Fig. 4 shows how the patches are feeding by power division lines. Transmission lines divides into two branches and each branch divides again until it reaches the patch elements. For a broadside array all the divided lines are of the same length. A disadvantage of parallel feeding is that the insertion loss is higher than that of a series feeding, however is less affected by phase changes due frequency changes, because relative phases between all elements will remain the same. The corporate feed array can achieve a bandwidth of 15% or more, depending on the design.

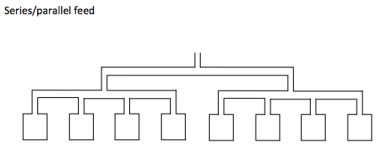

Fig. 5. Series-Parallel feed configuration for microstrip arrays. After (Lee, 1997)

The hybrid series/parallel array is shown in Fig. 5 where a combination of series and parallel feed lines are used, feeding elements in this way is possible to have a wider bandwidth than the series feed array but with a higher insertion loss due the parallel feeding, but the technique allows to make design trade-offs between bandwidth and insertion loss.
A microstrip can be designed in a single layer or multilayer configuration, decision is related with complexity and cost, sidelobes, cross polarization, bandwidth and other factors. Using a single layer reduces manufacturing costs but other characteristics are degraded. When low sidelobe or cross polarization is needed the double layer design seems to be the better choice. Fig. 6 shows a multilayer of a dual polarization antenna, where the antenna feeding is obtained with crossed slots on the ground plane and the feeding of the two polarizations is obtained using two orthogonal microstrip lines. A disadvantage of planar arrays is the influence between elements and feed lines, which affects the performance of the others, then in the design is very important to take into account effects as mutual coupling and internal reflections; coupling between elements generates surface waves within the substrate which can be eliminated using cavities in conjunction with microstrip feeding elements, but these effects are difficult to analyze for common analytical methods, therefore for accurate results should be used full wave solutions as those presented in this chapter, applied in most of the actual computational tools of present days.

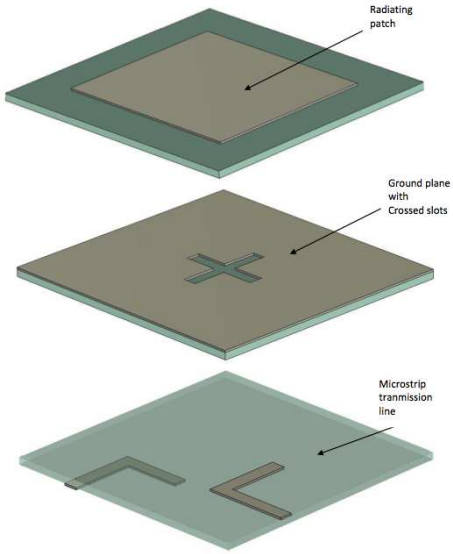

Fig. 6. Multilayer dual-polarized microstrip patch element. After (Lee, 1997)

4. Computational Tools

At the beginning of 80's, when the boom of planar antennas started the only available computational tools where the CAD packages, but their applications were constrained to low frequency electronic systems (Harrington, 1992) and the microwave programs were limited and expensive. The situation has changed radically since the arrival of personal computers and mainly the permanent improvement of their characteristics, making them a powerful tool for analysis of electromagnetic problems; on the other hand, the use of mathematical models had become in the development of specialized software tools widely used nowadays in the field of planar antenna analysis and design. Although the appearance of many commercial tools is a common situation every day, many researchers use their own programs; authors have been working since some years ago in development of their own software, applying it to antenna and microstrip devices (Barrera-Figueroa et al., 2007; 2009; Sosa-Pedroza et al., 2008; 2009) considering both, saving economical resources and "learning doing" mainly for academic reasons. Most of the actual work on antenna computational methods is based on solution of Maxwell Equations in integral or differential form, Method of Moments is an example and maybe the most applied for integral Methods and Finite Elements (FE) and Finite Difference on Time Domain (FDTD) for differential methods.

4.1 Method of Moments (MoM)

Integral Methods solve Maxwell's Equations in its integral form, describing the electromagnetic problem. As the current density on the conductor is related with the Electric Field, some equations have been derived from Maxwell equations, two examples of those are Pocklington equation and Hallén Equation, both can be studied in the literature (Balanis, 2005; Kraus et al., 2002). For an arbitrary shaped wire (Sosa-Pedroza et al., 2007) as the one shown in Fig. 7, is possible to deduce Pocklington Equation given by:

$$E_s^I = -\frac{j}{\omega\epsilon}\int_s' I_s(s')\left[k^2\mathbf{s}\cdot\mathbf{s} + \frac{\partial^2}{\partial s\partial s'}\right]\frac{e^{-jkr-r'}}{4\pi r - r'} \tag{31}$$

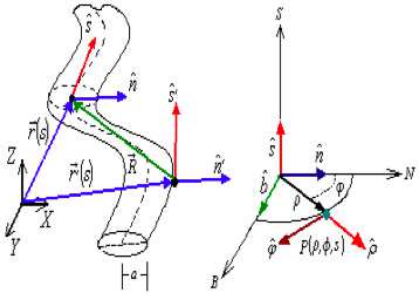

Fig. 7. Arbitrary shaped wire

E_s^I is the tangential incident electric field. As it seen the unknown distribution current is inside the integral and solution is not possible. The MoM formulation, introduced by Harrington in the 60's (Harrington, 1961), is used to get a numerical solution of (31) expressing the unknown function as a linear combination of n linearly independent functions, called basis functions:

$$I_s(s') = \sum_{n=1}^{N} c_n i_n(s') \tag{32}$$

where c_n are the unknown coefficients to be determined. Substituting (32) into (31) results the equation with N unknowns:

$$E_s^I = -\frac{j}{\omega\epsilon}\sum_{n=1}^{N} c_n \int_s w_m \int_{s'} i_n(s')\left[k^2\mathbf{s}\cdot\mathbf{s} + \frac{\partial^2}{\partial s\partial s'}\right]\frac{e^{-jkr-r'}}{4\pi r - r'} \tag{33}$$

with $m = 1, 2, ..., N$.
for a consistent equation system, is necessary to find N linearly independent equations, then is used the inner product of (33) with other set of N chosen linearly independent functions $w_m(s)$ named weight function, then

$$\int_s E_s^I ds = -\frac{j}{\omega\epsilon}\sum_{n=1}^{N} c_n \int_s w_m \int_{s'} i_n(s')\left[k^2\mathbf{s}\cdot\mathbf{s} + \frac{\partial^2}{\partial s\partial s'}\right]\frac{e^{-jkr-r'}}{4\pi r - r'} \tag{34}$$

Which can be reduced in a matrix form as:

$$\begin{pmatrix} Z_{11} & Z_{12} & \dots & Z_{1N} \\ Z_{21} & Z_{22} & \dots & Z_{2N} \\ \vdots & \vdots & \ddots & \vdots \\ Z_{N1} & Z_{N2} & \dots & Z_{NN} \end{pmatrix}\begin{pmatrix} c_1 \\ c_2 \\ \vdots \\ c_N \end{pmatrix} = \begin{pmatrix} v_1 \\ v_2 \\ \vdots \\ v_N \end{pmatrix} \tag{35}$$

where the elements Z_{mn} are obtained from:

$$Z_{mn} = -\frac{j}{\omega\epsilon}\int_s w_m \int_{s'} i_n(s')\left[k^2\mathbf{s}\cdot\mathbf{s} + \frac{\partial^2}{\partial s\partial s'}\right]\frac{e^{-jkr-r'}}{4\pi r - r'} \tag{36}$$

and the elements v_m are:

$$v_m = \int_s w_m E_s' ds \tag{37}$$

c_n represent the system's unknowns. Matrices of (35) are known as impedance matrix (Z_{mn}), current matrix (c_n), and voltage matrix (v_m). The solution for (35) is:

$$(c_n) = [Z_{mn}]^{-1}(v_m) \tag{38}$$

where the inverse matrix$(Z_{mn})^{-1}$ is obtained by a numerical technique. It is important to mention that both, basis and weight functions are arbitrary functions, selected considering computational resources and time and accuracy of solution. As is seen the Kernel of the integral includes Green's function, representing the electromagnetic influence on the entire surrounding space. Solution is valid at every point of an infinite space, including the far field radiation phenomena that are vital for antenna analysis.

Integral equations are established as a multilayered Green's function, such that the background can consist of an arbitrary number of horizontal, infinitely stretched layers, containing dielectric substrates and conducting ground planes, always present on planar antennas. The main components on the antenna are replaced with equivalent surface/volume currents, appearing as the primary unknowns in the resulting integral equations, solved by MoM. From (35) we can see that the method creates a dense matrix equation which solution gives the current distribution on the environment, after that, all other antenna parameters are easily obtained.

4.2 Finite Difference on Time Domain (FDTD)

Differential methods solve Maxwell Equations in their differential form; most of the computational solvers use the Finite Element Method (FEM) and the Finite Difference on Time Domain (FDTD).

The FDTD method, introduced by (Yee, 1966), transforms the Differential Maxwell Equations in Finite Difference Equations, used to generate an algorithm and a program code to solve them, over a specific propagation region; it uses the Yee's cell algorithm in a central difference scheme, considering field variations in time and space as the original Maxwell Equations, the characteristics of media are also defined in the method by means of ϵ, μ and σ characteristics, the algorithm is processed by a computer to analyze behavior of EM field moving over an environment of any kind. The interacting electric and magnetic fields are given by:

$$\frac{\partial H_x}{\partial t} = \frac{1}{\mu}\left[\frac{\partial E_y}{\partial z} - \frac{\partial E_z}{\partial y} - (M_{source_x} + \sigma^* H_x)\right] \tag{39}$$

$$\frac{\partial H_y}{\partial t} = \frac{1}{\mu}\left[\frac{\partial E_z}{\partial x} - \frac{\partial E_x}{\partial z} - (M_{source_y} + \sigma^* H_y)\right] \tag{40}$$

$$\frac{\partial H_z}{\partial t} = \frac{1}{\mu}\left[\frac{\partial E_x}{\partial y} - \frac{\partial E_y}{\partial x} - (M_{source_z} + \sigma^* H_z)\right] \tag{41}$$

$$\frac{\partial E_x}{\partial t} = \frac{1}{\epsilon}\left[\frac{\partial H_z}{\partial y} - \frac{\partial H_y}{\partial z} - (J_{source_x} + \sigma E_x)\right] \tag{42}$$

$$\frac{\partial E_y}{\partial t} = \frac{1}{\epsilon}\left[\frac{\partial H_x}{\partial z} - \frac{\partial H_z}{\partial x} - (J_{source_y} + \sigma E_y)\right] \tag{43}$$

$$\frac{\partial E_z}{\partial t} = \frac{1}{\epsilon}\left[\frac{\partial H_y}{\partial x} - \frac{\partial H_x}{\partial y} - (J_{source_z} + \sigma E_z)\right] \tag{44}$$

These equations are transformed in a discrete form using the Yee algorithm, which can be solved by computational methods, as an example is presented only one of them:

$$\frac{E_x\,|^{n+1/2}_{i,j+1/2,k+1/2} - E_x\,|^{n-1/2}_{i,j+1/2,k+1/2}}{\Delta t} = \frac{1}{\epsilon_{i,j+1/2,k-1/2}} \cdot$$
$$\left\{ \frac{H_z\,|^{n}_{i,j+1,k+1/2} - H_z\,|^{n}_{i,j,k+1/2}}{\Delta y} - \frac{H_y\,|^{n}_{i,j+1/2,k+1} - H_y\,|^{n}_{i,j+1/2,k}}{\Delta z} \right.$$
$$\left. - J_{source_x}\,|_{i,j+1/2,k+1/2} - \sigma_{i,j+1/2,k+1/2} E_x\,|_{i,j-1/2,k+1/2} \right\} \tag{45}$$

Yee Algorithm discretizes both time and space, represented by parameters n, i, j, k with intervals of Δt and Δ respectively. As seen in equation (45) the media characteristics are specially considered as ϵ, μ and σ which position is defined using the (i, j, k) subindex, then is possible to analyze the effects of any material at any position on the computational space. A computational code of any program language permits to know the EM behavior over the entire computational space. The FDTD and also the FE differential-equation methods are particularly suitable for modeling full three-dimensional volumes that have complex geometrical details. They are extremely efficient for smaller close-region problems involving inhomogeneous media (James et al., 1989).

4.3 Computational tools comparison

An excellent summary and comparison of actual available commercial software used on planar antenna analysis and design is presented in (Vasylchenko, 2009), they analyze 5 commercial tools and one "in house", comparing all of them in the analysis of planar antennas looking to guarantee the optimal use of each of the software packages, to study in detail any discrepancies between the solvers, and to assess the remaining simulation challenges. Even their work is not the first one on the theme, mentioning references strengthening their vision that, an extensive benchmark study over a large variety of solvers and for several structures has not yet been documented.

As the operation of EM solvers is based on the numerical solution of Maxwell's equations in differential or integral form, one or other influences the efficiency and accuracy and users may get the wrong impression that a given solver is automatically suited to solve any kind of problem with arbitrary precision. Comparison in the Vasylchenko work verifies the plausibility of such expectations by presenting an extensive benchmark study that focuses on the capabilities and limitations of the applied EM modeling theories that usually remain hidden from the antenna designer. The integral solvers they analyze are the one they designed in K. U. Leuven's: MAGMAS 3D, the others are IE3D from Zeland Software, FEKO from EM Software & Systems, and ADS Momentum from Agilent. On the other hand they analyze the two leading differential EM tools, HFSS from Ansoft for the finite-element method, and CST Microwave

Studio for the FDTD method. After a careful analysis, comparing results with measurement of 4 common planar antennas, their conclusion is as follows:
Classical patch antennas could be predicted by every simulation program with a deviation not beyond 1.5 %. The simulation based on MoM was inherently faster and are more attractive in price. On the other hand the FEM and FDTD are inherently able to analyze much more general structures, but require the inversion of much larger, but sparse, matrices, requiring higher memory resources. Although the calculation times were not that different at the time of experiment, they presented a reference in which it seems that dedicated inversion techniques for MoM solvers are nowadays fully in development, opening the possibility that better times can be obtained for differential equations solvers.
Proper mesh generation and a correct feeding model are two crucial issues predetermining the successful simulation in the software packages reviewed. In general, a very neat adaptive mesh refinement, implemented in Ansoft's HFSS and as an option in CST's MWS, allows better handling of a design with difficult electromagnetic coupling between its different parts. Such characteristics pertain to applications in mobile gadgets, such as the GSM antennas. Having no mesh refinement option, MoM-based programs require more careful consideration of the initial meshing. MoM solvers can provide an improvement in simulation results and time using so called edge-meshing features, while avoiding excessive meshing on the bulk of the metal structure. However the study concludes that the meshing schemes in all solvers are adequate.
Some designs, such as the GSM and UWB antennas, require finite substrate effects to be taken into account, such as diffraction from substrate edges. MoM based solvers show better convergence when a dielectric substrate is infinite, but the trend toward miniaturizing antennas diminishes the advantage of using these solvers, then they conclude that at present, differential equations programs are better suited for modeling small antennas. On the other hand(Vasylchenko, 2009) suggest that the feeding models, as implemented today in the widespread commercial 35 solvers, are probably unsatisfactory in the case of small structures with complicated electromagnetic-coupling behavior, but HFSS and CST MWS solvers are better suited to handle the problem.
As a final guideline, authors recommend the use of two different solvers, based on different theoretical methods (integral and differential), to characterize a specific device if both results are in good agreement, it is reasonable to expect that the results can be trusted, if the two results are in disagreement, a deeper investigation of the structure and its modeling is absolutely necessary.

5. Planar antennas on space applications

When a designer decide to use planar or microstrip antennas on a space applications should take in account three factors among those related with the inherent design of the radiator (Lee, 1997); those factors are critical and need to be considered. One is that the antenna must be able to support the high vibration produced during the launch from the Earth; acceleration can be as high as 10 Gs or more, under this conditions soldering junctions and laminating of multilayer antennas tend to breakdown, then they should be made strong enough to survive the vibration, a solution could be the use of noncontacting feeds as proximity, capacitive or aperture coupling. The second factor is related with the extreme temperature difference which can be as high as 100°C to -70°C, whether the antenna "sees" the sun or not, behind a shaded area. Under this condition, the laminating adhesive material must survive physically and electrically into this environment. Third factor is the space vacuum, as is known at low

pressures, electrons are almost free to leave an electrode and move across to the opposite electrode, a phenomenon known as multipacting. For a microstrip antenna, the two electrodes are the patch and the ground plane, when the phenomenon is present reduces the capacity of power handling of the antenna then it should be designed with the proper thickness. These three factors limit the use of planar and especially microstrip antennas, nevertheless there are many examples of spacecrafts which can be mentioned: Earth Limb Measurements Satellite, Shuttle Imaging Radar, Geostar system and especially the Mars Pathfinder using a small X band microstrip antenna providing circular polarization with a peak gain of 25 dB. Antenna was constructed with a parallel feed power divider and electromagnetically coupled dipoles. The divider and the dipoles were printed on multilayer honeycomb substrates which have open vented cells for space applications.

5.1 Morelos: First Mexican Satellite System

Historically the first satellites using planar antennas could be the Mexican Morelos System, constructed by Hughes Aircraft Company (Satmex, 2010);. They were launched on the space Shuttle in June 17 and November 27, 1985 and they were the first in use the HS-376 platform as a hybrid satellite operating in two frequency bands (C and Ku) simultaneously. The four Ku-band channels used the planar arrays for reception only having a bandwidth of 108 MHz with a minimum effective isotropic radiated power (EIRP) of 44 dBW throughout Mexico. Transmit and receive beams in the C-band and the transmit beams in the Ku-band were created by a 1.8 m wide shared aperture grid antenna with two polarization-selective surfaces. The front surface was sensitive to horizontally polarized beams and the rear was sensitive to vertically polarized beams. Separate microwave feed networks are used for the two polarizations. Fig. 8(a) shows the spacecraft with the planar array and Fig. 8(b)the antenna and the reflector in the construction bay. Morelos Satellites were a very successful communications system; Morelos 1 exceeded his life from 9 years to 10, when it was substituted in 1996 for the first satellite of 2^{nd} generation of Mexican satellites, but Morelos 2 was in operation until to 2002, almost doubling its life designed time.

5.2 The IRIDIUM Main Mission Antenna Concept

A commercial satellite system using planar antennas is the MOTOROLA's IRIDIUM (Schuss et al., 1990) shown in Fig. 8(c) used for personal satellite communications with a constellation of 66 satellites placed in low earth orbit, positioned in six polar orbital planes with 11 satellites plus one spare per plane. The main mission antenna (MMA), consists of three fully active phased-array panels providing the band link from the satellite to the ground user. Each phased-array panel produces 16 fixed simultaneous beams for a total of 48 beams per satellite linked to hand-held phones having low-gain antennas. The MMA radiates multiple carriers into multiple beams with high efficiency and linearity as well as being lightweight and able to function in the thermal and radiation environment of space. MMA was optimized for the highest link margin accordingly with its size and the budgeted RF power per carrier. The architecture of the MMA phased-array panel is shown in Fig. 8(d); each array consists of over 100 lightweight patch radiators, each of which is driven by a Transmitter/Receiver (T/R) module, which are in turn collectively excited by an optimized beamformer network. The beamformer network forms the 16 optimized shaped beams for both transmit and receive operation with the T/R modules maintaining a high G/T in receive operation and efficient EIRP generation for transmit operation. The satellite can receive or transmit through each beamport, providing the RF access to a particular fixed beam. In general, several or all beams

(a) The *Morelos* satellite

(b) The *Morelos* at the construction bay

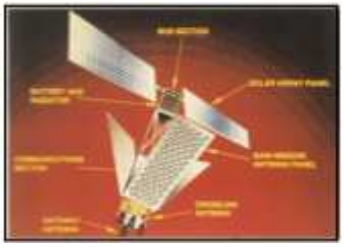

(c) IRIDIUM space vehicle (©(1999) IEEE)

(d) MMA panel construction (©(1999) IEEE)

Fig. 8. The use of planar antennas in commercial satellites and space vehicles

can be utilized at once in either transmit or receive operation with the only limitation being the MMA capacity constraints on transmit.

5.2.1 Patch Radiator

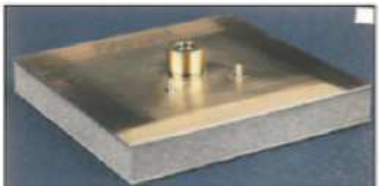

(a) Bottom view of patch radiator (©(1999) IEEE)

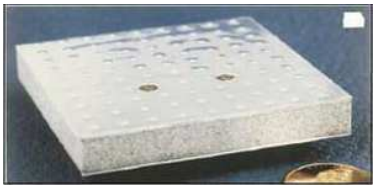

(b) Top view of patch radiator (©(1999) IEEE)

Fig. 9. Patch radiator developed for the MMA

Fig. 9(a) and Fig. 9(b), show the patch radiator developed for the MMA, which was manufactured as a separate component and bonded onto the MMA panel during array assembly; its radiator is built as one assembly and contains the matching and polarizing networks; a single 50 Ω input connector is provided on the underside of the patch for connection to the T/R module. The radiator cavity is loaded with an artificial dielectric substrate whose weight is approximately one tenth that of teflon, but which has a dielectric constant of approximately two. This dielectric constraint is needed to obtain the desired scan and polarization performance of the array. The artificial dielectric also permit efficient heat radiation out the front face of the array during peak traffic loads.

5.3 Antennas for Modern Small Satellites

Many examples of planar antennas application are discussed in literature, but its major application could be the modern small satellites (MSS) which are revolutionizing the space industry (Gao et al., 2009). They can drastically reduce the mission cost, and can make access to space more affordable.

These modern small satellites are useful for various applications, including telecommunications, space science, Earth observation, mitigation and management of disasters (floods, fire, earthquake, etc.), in-orbit technology verification, military applications, education, and training. Typical antenna coverages ranges from low-gain hemispherical, to medium-gain antennas. The basic radiator designs used are normally helices, monopoles, patches, and patch-excited cups (PEC), depending on frequency and range, coverage requirements, and application. As antenna examples of small satellites are mentioned various monopole antennas, printed inverted-F-shaped antennas (PIFAs), microstrip-patch antennas, helices, and patch-excited cup antennas, developed for telemetry, tracking, and command in the UHF, VHF, S, C, and X bands. These antennas are simple, cheap, easy to fabricate, and have wide radiation-pattern coverage; the satellite thus does not need accurate control of attitude.

Universities have played an important role in satellites development, since the beginning of space era; professors were interested in the new research area, either as academic developers or as a part of contracts with satellite industry, but small satellites seems to be a very appropriate area to be working in by universities, due the few economical resources needed. As an example we can mention universities in Mexico, creating clusters to design small satellites; institutions as CICESE (Centro de Investigación Científica y de Educación Superior de Ensenada) in north of Mexico developing transponders and the Instituto Politécnico Nacional working with satellite structures and integration into a clean room, design of monopoles and planar antennas for satellite applications and also exploring the capabilities of new active devices as candidates for LNA amplifiers (Enciso et al., 2005). An especial mention should be make to the Universidad Nacional Autónoma de México (UNAM) which has been working towards the design of a femto satellite.

Other illustrative example is the University of Surrey, which has been developing modern small satellite technology since starting its UoSAT program in 1978. UoSAT-l, developed by Surrey, was launched in 1981. This was followed by UoSAT-2 in 1984. UoSAT-l continued to operate for eight years, while UoSAT-2 was still operational after 18 years in orbit. During the past 30 years, the University of Surrey's spinoff company, Surrey Satellite Technology Ltd. (SSTL), together with Surrey Space Centre (SSC), have successfully designed, developed and launched 32 modern small satellites for various countries around the world. (Gao et al., 2009) have a complete description of various small satellites, which are described in the next lines and figures. Fig. 10 shows a photograph of the S-band microstrip-patch antenna used at SSTL;

it employs a circular microstrip patch, fed by a 50Ω probe feed at the bottom. It can operate within a tunable frequency range of 2.0-2.5 GHz. Left-hand or right-hand circular polarization can be achieved by using a single feed combined with patch perturbation, or a 90°microstrip hybrid combined with a circular patch. It achieves a maximum gain of about 6.5 dBi, has a size of 82 x 82 x 20 mm, and a mass of less than 80 g. It can operate within -20°C to +50°C, is radiation tolerant to 50 kRad, and qualified to 50 Gs rms random vibration on three axes.

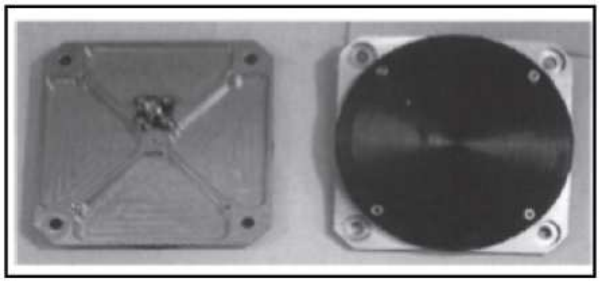

Fig. 10. An S-band patch antenna SSTL. (©(2009) IEEE)

To respond the need for single-frequency low-profile and low-weight hemispherical or near-hemispherical antennas, working at S, C, or X band, patch-excited cup antennas were developed at RUAG Aerospace Sweden. They consist of a short cylindrical cup, with a circular cross section and an exciter. The cup is excited using a stacked circular dual-patch element, or a single patch. The lower patch or the single patch is fed at one point, and the patch has two opposite perturbations for generating circular polarization. The antennas have special features to minimize their coupling to the surrounding spacecraft environment, as this is a common problem for low-gain antennas of this type, and it has an effect on the installed performance. The antenna's diameter is 60 mm for the C band antenna, and 40 mm for the X-band antenna. The mass is less than 90 g for the C-band antenna, and less than 20 g for the X-band antenna. They are both almost all metal antennas (which is a preferred property), with dielectric material only in the interface connector.
Fig. 11 shows the X-band patch-excited cup antennas that can be used for the telemetry, tracking, and command function. Fig. 12(a) shows the S-band patch-excited cup antenna, developed at Saab Space. It consists of three patches, mounted within a thin aluminum cup with a rim height of about a quarter wavelength. Two lower patches form a resonant cavity, allowing broadband or double tuning. The top patch acts as a reflector that affects the illumination of the aperture, and is used to improve the aperture efficiency. To achieve circular polarization, the lower patch is fed in phase quadrature at four points by a stripline network. It achieves a maximum gain of about 12 dBi. A patch-excited cup antenna development performed at Saab Space is the update of the antenna in Figure 6, to be used for other missions; it has a radiator tower that is modified compared to the original design. It is now an all-metal design, and has a new feed network configuration: an isolated four-point feed design, antenna is shown in Fig. 12(b).
Surrey also pioneered the use of GPS and global navigation satellite systems (GNSS) in space. A GPS receiver can provide accurate position, velocity, and time for LEO satellites. For this application, the antenna needs to be compact, low profile, able to operate at GPS frequencies in the L1 (1.575 GHz) and L2 (1.227 GHz) bands with stable performance, and produce low backward radiation towards the small satellite body.

Fig. 11. An X-band patch-exited cup antenna (©(2009) IEEE).

A medium-gain antenna, shown in Fig. 13(a), was launched on the UK-DMC satellite of SSTL for the purpose of collecting reflected GPS signals in orbit. This satellite has begun to collect reflected signals under a variety of sea conditions, and over land and ice. The antenna is a three-element, circularly polarized microstrip-patch array with a gain of 12 dBi. Antenna-design challenges remain in terms of further reducing antenna size, improving the antenna's efficiency, multi-band (L1/L2/L5 band) operation, constant phase center, multipath mitigation, etc.
Fig. 13(b) shows the patch-excited cup antenna developed at RUAG Aerospace Sweden. It consists of two patches placed in a circular cup. To obtain a stable antenna covering two GPS frequency bands (Ll, L2), the bottom patch was capacitively fed by four probes and an isolated feed network. The antenna achieved a coverage out to 80^0 in zenith angle, and low backward radiation. The antenna's diameter is 160 mm, and the mass is 345 g. This antenna shows how shorted-annular-patch can achieve high-accuracy GPS/GNSS performance without compromising the physical constrains.

6. Some proposals for future applications

Spacecraft development and research never ends and antenna improvements are not the exception, even thinking that some of them were designed for other applications, always is possible to extrapolate to space applications, but antenna research and design for satellites and spacecrafts is an area of permanent expansion. Starting with airborne applications, where planar antennas have a permanent development, to meet the low profile and conformal challenges, is possible to extrapolate them to satellite systems. For airplanes as for satellite and spacecrafts, an array antenna should have good isolation, high efficiency, and ease of integration, also a simple feeding-line network with lower loss and high isolation is generally desired. Microstrip series-fed arrays have been shown to have a structure that enhances the antenna's efficiency. This is because the array feeding-line length is significantly reduced, compared to

(a) Cup antenna at RUAG (©(2009) IEEE)

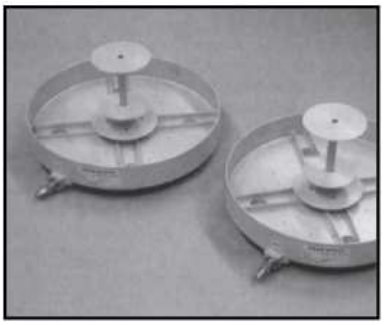

(b) Medium-dowlink antennas (©(2009) IEEE)

Fig. 12. S-band patch-excited cup antenna.

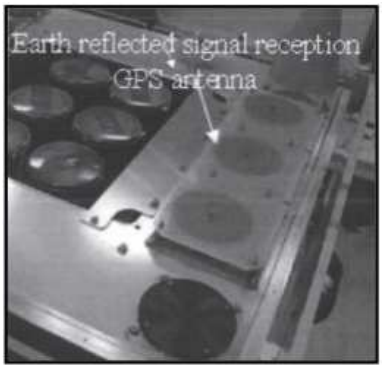

(a) For the UK DMC satellite at SSTL (©(2009) IEEE)

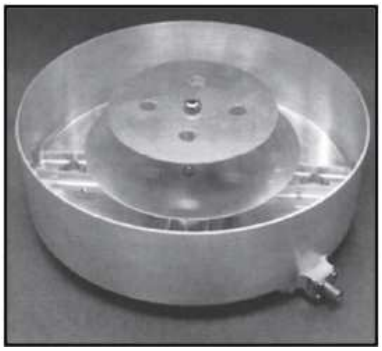

(b) Antennas at RUAG (©(2009) IEEE).

Fig. 13. GPS antennas.

the conventional corporate feeding-line network. A planar structure with a thin and flexible substrate is a good choice, because it will not disturb the appearance of the aircraft, and can be easily integrated with electronic devices for signal processing.

6.1 The Shih planar antenna

An example of a planar antenna first designed for aircrafts is the dual-frequency dual-polarized array antenna presented by (Shih et al., 2009). It consists of a multilayer structure of two antennas separated on different layers, adopted for dual-band operation, working in the S band and X band frequencies. To reduce the array's volume and weight, a series-fed network is used. An ultra-thin substrate is chosen in order to make the array conformal, and the array can be easily placed on an aircraft's fuselage, or inside the aircraft.

6.1.1 S-band Array Design

The multilayer array structure for dual-band operation is shown in Fig. 14. The S-band antenna elements sit on the top layer, and the X-band antennas are on the bottom layer. A foam layer (h_2) serves as the spacer, and is sandwiched between the two substrate layers. One of the important design considerations for this multilayer dual-band array is that the S-band antenna element should be nearly transparent to the X-band antenna elements. Otherwise, the S-band element may degrade the performance of the X-band antenna. Two RTlDuroid 5880 substrates (ϵ_1 =ϵ_3 =2.2) and a foam layer (ϵ_2 = 1.06) form the multilayer structure. The thicknesses of the substrates (h_1 and h_2) are both only 0.13 mm. These ultra-thin and flexible substrates make it possible for the array to be easily attached onto the aircraft's fuselage, or installed inside the aircraft. The foam layer has a thickness of h_2 =1.6 mm.

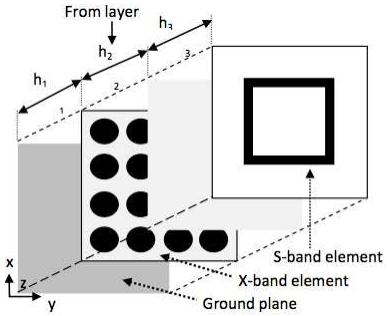

Fig. 14. The multilayer structure of dual-band dual polarized array antenna (©(2009) IEEE).

6.1.2 X-Band Antenna and Subarray

The X-band array uses the circular patch as its unit antenna element. The circular patches are fed with microstrip lines at the circumferential edge, as shown in Fig. 15(a) for a single circular patch, two microstrip feeding lines are used to feed the circular patch to generate two orthogonally radiating TM_{11} modes for dual polarized operation. Two feed points are located at the edge of the patch, 90ą away from each other, so that the coupling between these two ports can be minimized. The port isolation also depends on the quality factor of the patch. Increasing the substrate's thickness decreases the isolation, therefore using thin substrates could improve the quality of isolation.

Fig. 15(a) shows a 4 x 8 dual-polarized X-band array. The V port and the H port are the input ports for the two orthogonal polarizations (vertical and horizontal). The array is composed of two 4 x 4 subarrays. The corporate-fed power-divider lines split the input power at each port to the subarrays. Within each subarray, the circular patches are configured into four 4 x 1 series-fed resonant type arrays, which make the total array compact and have less microstrip line losses than would a purely corporate-fed type of array. An open circuit is placed after the last patch of each 4 x 1 array. The spacing between adjacent circular-patch centers is about one guided wavelength (λ_g =21.5 mm at 10 GHz). This is equivalent to a 360^o phase shift between patches, such that the main beam points to the broadside. The power coupled to each patch can also be controlled by adjusting the size of the individual patch to achieve a tapered amplitude distribution for a lower-sidelobe design.

As shown in Figure Fig. 15(b), the S-band antenna elements are printed on the top substrate, and are separated from the X-band elements by the foam layer. To reduce the blocking of

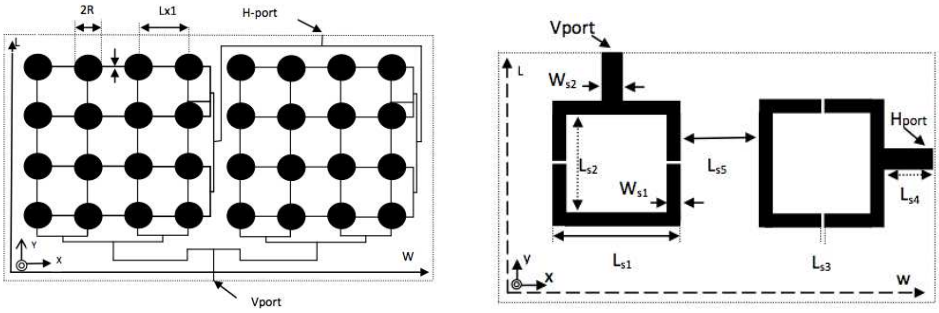

(a) X-band antenna (©(2009) IEEE) (b) S-band antenna (©(2009) IEEE)

Fig. 15. Microstrip Antenna Arrays

the radiation from the X-band elements at the bottom layer, the shape of the S band elements has to be carefully selected. A ring configuration was a good candidate, since it uses less metallization than an equivalent patch element. Here, a square-ring microstrip antenna is used as the unit element of the S-band array. Because antenna elements at both frequency bands share the same aperture, it is also preferred that the number of elements on the top layer be as small as possible, to minimize the blocking effects.

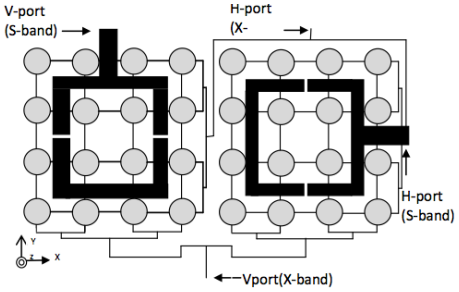

Fig. 16. Geometry of dual antenna (©(2009) IEEE)

The stacked X-band and S-band array antennas are shown in Fig. 16. As can be seen in the figure, the four sides of the square-ring element are laid out in such a way that they only cover part of the feeding lines on the bottom layer, but none of the radiating elements. Unlike an ordinary microstrip-ring antenna that has a mean circumference equal to a guided wavelength, the antenna proposed here has a mean circumference of about $2\lambda_g$ (λ_g = 82.44mm at 3 GHz). Although the size of the proposed unit element is larger than an ordinary ring antenna, its gain is about twice as high, because of its larger radiation-aperture area. The ring is loaded by two gaps at two of its parallel sides, these make possible to achieve a 50 Ω input match at the edge of the third side without using a small value of L_{s2}/L_{s1}. For an edge fed microstrip ring, if a second feed line is added to the orthogonal edge, the coupling between the two feeding ports will be high. The V-port and H-port feeds are therefore placed at two individual elements, so that the coupling between the two ports can be significantly reduced. Using separate elements seems to increase the number of antenna elements within a given aperture.

However, this harmful effect could be minimized by reducing the number of elements with the use of larger-sized microstrip rings.

6.2 The Cross Antenna

The cross antenna is another possibility of use in spatial applications, it is a traveling wave antenna with circular polarization formed by conductors over a ground plane, proposed by (Roederer, 1990). Antenna can be constructed as a wire or printed antenna. Roederer's paper do not describe completely the antenna but it was reanalyzed by authors (Sosa-Pedroza et al., 2006).

The cross antenna is a printed structure of medium gain and circular polarization, consisting of a conductor or microstrip over a ground plane following the contour of a cross with four or more arms and a diameter of about 1.5 wavelengths. The antenna is feeding on one end by a coaxial line and finished on the other end by a load impedance, considering behavior of travelling wave. Even the antenna was primarily designed for applications in L Band (1500 MHz) mobile communications, the design and experimental characterization was made at 10 GHz and for an eight arms antenna besides original four arms antenna, showing the possibility of extrapolation for other applications as satellite communications. For the cross antenna, feed connector and load position define the right or left circular polarization; it can be used as a unique radiator or as a part of an array, a proposal is that could be used as primary antenna for parabolic reflector with wide focal length and diameter relationship. The main advantage of the cross antenna is its gain (12-15 dBi) compared with its size and weight, ideal for space communications.

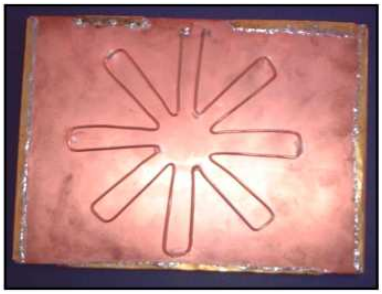

Fig. 17. The cross wire antenna

Arm length	λ_{eff}
Arm width	$0.25\lambda_{eff}$
Cross diameter	$2.5\lambda_{eff}$
Wire diameter	$0.01\lambda_{eff}$

Table 2. Geometric characteristics of cross antenna

The power at the end of the antenna is controlled by the load impedance and is limited to a small percentage, changing the height of the conductor over the ground plane (typically $\lambda_{eff}/20$ to $\lambda_{eff}/4$) which also affects the axial rate. The bandwidth of the cross antenna is around 5% depending on the number of arms. Fig. 17 shows photograph of a 8 arm radiator,

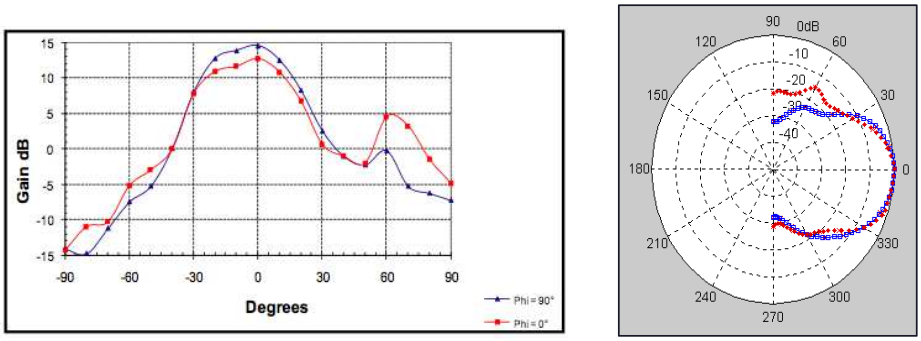

(a) Gain (b) Radiation Pattern

Fig. 18. Electrical characteristics of the Cross antenna

which was constructed both, as a microstrip antenna using a 3.6 mm thick RTDuroid with 2.3 of ϵ_{eff}=2.3 and as a wire antenna using copper wire, supported over the ground plane by small Teflon fragments giving flexibility to move up the structure to analyze the effect of height over the ground plane. Table 2 shows dimensions of the antenna. On the other hand Fig. 18(a) and Fig. 18(b) show the gain and the radiation pattern respectively, for one of the antennas.

6.3 Rhombic cross antenna

A variation over cross antenna is a four arm rhombic cross antenna (Lucas et al., 2008), it is also a medium gain and circular polarization structure made of a conductor or strip line over a ground plane, following a rhombic contour of four branches. One end is connected to the feed line and the other is grounded by a load impedance. Antenna was analyzed using Method of Moments and constructed for experimental analysis using both, a 12 AWG wire over a ground plane and printed as a microstrip structure working in 4.2 GHz. The rhombic antenna shows a better performance compared with the four arms Roederer's antenna, with almost 15 dB gain and 1.4 dB for axial ratio. The antenna can be used in mobile communication or as primary radiator of parabolic reflectors, when circular polarization is needed. The construction repeatability is very easy as well the facility to obtain 15 dB gain in a very small antenna.

A	$0.430\lambda_{eff}$
B	$0.276\lambda_{eff}$
C	$0.3911\lambda_{eff}$
D	$1.4112\lambda_{eff}$

Table 3. Dimensions of rhombic antenna

The rhombic cross antenna geometry is shown in Fig. 19(a), and antenna dimensions as function of effective wavelength, are given in Table 3.
There were constructed several antennas, both wire (air dielectric) and strip line (fiber glass dielectric), the last one is shown in Fig. 19(b); wire antenna uses Teflon supports over the

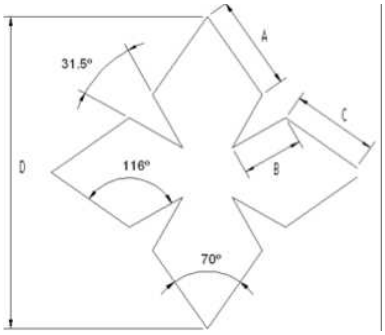

(a) Scheme of rhombic antenna

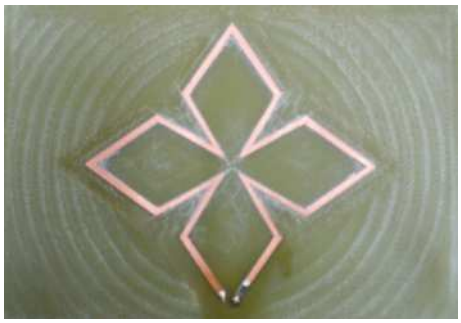

(b) Microstrip antenna

Fig. 19. Physical characteristics of Rhombic Antenna

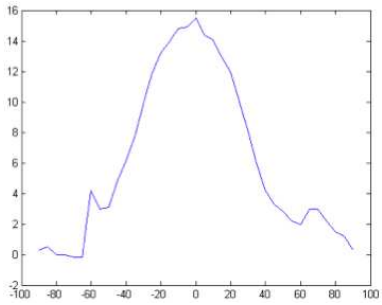

(a) Rhombic antenna gain

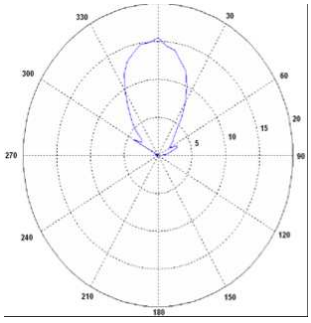

(b) Rhombic antenna field pattern

Fig. 20. Physical characteristics of Rhombic Antenna

ground plane, giving flexibility to change the height over it. Results for gain and field pattern are shown in Fig. 20(a) and Fig. 20(b) respectively, for a 50 Ω load impedance; the feed impedance is $Z = 38.6 - j56.8\Omega$ for 2.4 GHz:
Even the proposed antennas have not been used yet for spatial applications, their profiles can match for it, in frequencies ranging from L band, S band, commercial C band or X band, either as single structures or as arrays.

7. References

Agrawal, P. K., Bailey M. C. (1977) *An Analysis Technique for Microstrip Antennas*. IEEE Trans. on Antennas and Propagation AP-25, pp.756-759

Balanis, C.(2005).*Antenna Theory Analysis and Design*, Wiley-Interscience ISBN 0-471-66782-X

Barrera-Figueroa, V.; Sosa-Pedroza, J.; Lopez-Bonilla, J. (2007). *Numerical approach to King's analytical study for circular loop antenna*, Journal of Discrete Mathematical Sciences & Cryptography, Vol. 10, No. 1 February 2007, pp 82-92.

Barrera-Figueroa, V.; Sosa-Pedroza, J.; Lopez-Bomilla, J. (2009) *Pocklington Equation via circuit theory* Apeiron, on line Journal, Vol 16, No. 1.

Chang, K.(1989). *Handbook of Microwave and Optical Components*. Vol. 1, John Wiley & Sons, New York, USA

Derneryd, A.,G.(1975). *Linear Polarized Microstrip Antennas*. IEEE Trans. on Antennas and Propagation, AP-24, pp. 845-850.

Deschamps, G. A. (1953) *M*icrostrip microwave antennas. *3rd USAF Symposium on Antennas*.

Enciso-Agilar, M.; Crozat, P.; Hackbarth, T; Herzog, H,; Aniel F.(2005). *Microwave Noise Performance and Modeling of SiGe-Based HFETs*. IEEE Trans. on Electron. Dev., Vol. 52, No. 11, November 2005

Gao S.; Clark K.; Unwin M.; Zackrisson J.; Shiroma W.A.; Akagi J.M.; Maynard K.; Garner P.; Boccia L.; Amendola G.; Massa G.; C. Underwood; Brenchley M.; Pointer M.; Sweeting M.N. (2009). *Antennas for Modern Small Satellites.* IEEE Antennas and Propagation Magazine (August 2009), Vol. 51 No.4, pp. 40-56. IEEE. ISSN 1045 9243/2009.

Greig D., D.; Engleman H., F. (1952) Microstrip a new transmission technique for the kilomegacycle range. *Proceedings of IRE*, No. 40.

Gupta,K.C.; Benalla, A. eds. *Microstrip Antenna Design*. Artech House, Norwood MA, USA

Harrington, R.F.,(1961). *Time-Harmonic Electromagnetic Waves*, McGraw-Hil, New York, USA

Harrington,F.,R., *Matrix Methods for Field Problems*, Proc. IEEE, Vol. 55, No. 2, Feb. 1967.

Roger F. Harrington, (1992). *Field Computation by Method of Moments*, IEEE Press Series on Electromagnetic Waves, ISBN 0 7803 1014 4, Piscataway, NJ, USA.

Hirasawa, K.; Haneishi, M. (1994). *Analysis, Design and Measurement of Small and Low Profile Antennas*, Artech House, ISBN 0-89006-486-5,USA

Howell, J., Q.(1975) *Microstrip Antennas*. IEEE IEEE Trans. on Antennas and Propagation, vol. AP22 , pp. 74-78.

Itoh, T.; Menzel,W. (1989) *A Full Wave Analysis Method for Open Microstrip Structures*. IEEE Trans. on Antennas and Propagation AP-29 , 63-68.

James, J.R., Hall, P. S. (1989). *Handbook of Microstrip Antennas*, Vol 1. Peregrinus Ltd, IEE Electromagnetic Waves Series, ISBN 0 86341 150 9 Peter, London United Kingdom.

James, J. R.; Hall, P., S.; and Wood, C. (1981). *Microstrip antenna theory and design.* IEE Peter Peregrinus.

Kraus, J.,D.; Marhefka, R.,J. (2002) *Antennas 3rd. Edition*, ISBN 0 07 232103 2, New York NY USA.

Lee H.,F.; Chen, W. (1997). *Advances in Microstrip and Printed Antennas*. John Wiley & Sons, New York, USA

Long, S., A.; Shen, L.,C.; & Morel,P.,B. (1978). *A Theory of the Circular Disk Printed Circuit Antenna*. Proc IEE, Pt. H, Vol. 125, October 1978, pp. 925-928

Lucas-Bravo A., Sosa-Pedroza J., Barrera-Figueroa V. (2008). Experimental and numerical results of a rhombic cross antenna. *5o Congreso Internacional de Ingeniería Electromecánica y de Sistemas*, pp. 1178-1182. Mexico D.F., November 2008.

Thomas, A., Milligan.(2005). *Modern Antenna Design*. John Wiley & Sons. New Yersey, USA

Munson, R., E. (1974). "Conformal Microstrip Antennas and Microstrip Phased Arrays" *IEEE Trans. Antennas and Propagation*, Vol. AP-22, January 1974, pp 74-78, ISSN 0018-926X

Pozar,D.,M. (1982) *Input impedance and mutual coupling of rectangular microstrip antennas*. IEEE Trans Antennas Propagatation. AP-30, 1191-1196.

Pozar,D.M. (2005). *Microwave Engineering*, John Wiley & Sons, USA

Reineix, A.; Jecko, B. (1989) *Analysis of Microstrip Patch Antennas Using Finite-Diference Time Domain Method*. IEEE Trans. on Antennas and Propagation AP-37 pp. 1361-1369.

Richards,W.,F.; Lo,Y., T.; Harrison, D.,D. (1979) *An improved theory for microstrip antennas* .Electron. Letters, Vol 15 , 42-44.

Richards,W.,F.; Lo,Y., T.; Harrison, D.,D. (1981) *An improved theory for microstrip antennas and applications*. IEEE Trans. on Antennas and Propagation AP-29 , 38-46.

Roederer A. (1990). *The Cross Antenna: a New Low Profile Circularly Polarized Radiator*. IEEE Transactions on Antennas and Propagation, Vol. 38, no. 5, May 1990.

Schuss J. J., Upton J., Myers B., Sikina T., Rohwer A., Makridakas P., Francois R., Wardle L., and Smith R. (1999). *The IRIDIUM Main Mission Antenna Concept*. IEEE Transactions on Antennas and Propagation, Vol. 47, No. 3, March 1999, pp. 416-424, IEEE, ISSN 0018 926X/99

Sheen, D.,M.; Ali, S.,M.;Abouzahra M.,D.; Kong J.,A. (1990). *Application of Three-Dimensional Finite-Difference Time-Domain Method to the Analysis of Planar Microstrip Circuits*. IEEE Trans. on Microwave Theo. and Tech. vol. 38, pp. 849-857

Shih-Hsun H., Yu-Jiun R., and Kai C. (2009). *A dual-Polarized Planar-Array Antenna for S-Band and X-Band Airbone Applications.* IEEE Antennas and Propagation Magazine, Vol. 51, No.4, August 2009, pp.70-78

Sosa-Pedroza J., Lucas-Bravo A., Lopez-Bonilla J. (2006). Numerical and Experimental Analysis for a Cross Antenna. *International Caribbean Congress on Devices, Circuits and Systems* pp 207-211, ISBN: 1 4244 0042 2, Playa del Carmen, Quintana Roo, Mexico, April 2006.

Sosa-Pedroza, J.; Enciso-Aguilar, M.; Benavides-Cruz, M. (2008). A 9 slots antenna designed by Chebyshev technique and modeled by Finite Difference Time Domain, *Proc. of 7th International Caribean Conference on Devices Circuits and Systems*, Cancun Quintana Roo, Mexico, April 2008, IEEE.

Sosa-Pedroza, J., Barrera-Figueroa,V., Lopez-Bonilla, J. Equidistant and non-equidistant sampling for method of moments applied to Pocklington Equation. *The 18th Annual IEEE International Symposium on Personal, Indoor and Mobile Radio Communications*, Cancun Mexico, 2007.

Sosa-Pedroza J.; Enciso-Aguilar, M.; Benavides-Cruz, M.; Nieto-Rodríguez, M.; Galaz-Larios, M. A parametric analysis of perfect matched layer model of Finite Difference Time Domain Method, *Proc. of PIERS* 2009, Moscow, Russia.

Vasylchenko, A., Schols, Y., De Raedt , W., and Vandenbosch, G. A. E. *Quality Assessment of Computational Techniques and Software Tools for Planar-Antenna Analysis*, IEEE Antennas and Propagation Magazine, Vol. 51, No.1, February 2009

Volakis, J.,L.; Chatterjee, A.; and Kempel, L.,C. (1998). *Finite element method for electromagnetics* IEEE Press, Chap. 7, 1998.

www.satmex.com. (2010)

Yee, K. S (1966). *Numerical solution of initial boundary value problem involving Maxwell's equations in isotropic media.* IEEE Trans. on Antennas and Propagation, vol. 14, pp. 302-307.

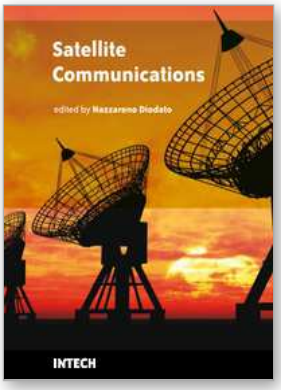

Satellite Communications

Edited by Nazzareno Diodato

ISBN 978-953-307-135-0
Hard cover, 530 pages
Publisher Sciyo
Published online 18, August, 2010
Published in print edition August, 2010

This study is motivated by the need to give the reader a broad view of the developments, key concepts, and technologies related to information society evolution, with a focus on the wireless communications and geoinformation technologies and their role in the environment. Giving perspective, it aims at assisting people active in the industry, the public sector, and Earth science fields as well, by providing a base for their continued work and thinking.

How to reference

In order to correctly reference this scholarly work, feel free to copy and paste the following:

Jorge Sosa-Pedroza, Fabiola Martinez-zuñiga and Mauro Enciso-Aguilar (2010). Planar Antennas for Satellite Communications, Satellite Communications, Nazzareno Diodato (Ed.), ISBN: 978-953-307-135-0, InTech, Available from: http://www.intechopen.com/books/satellite-communications/planar-antennas-for-satellite-communications

INTECH
open science | open minds

InTech Europe
University Campus STeP Ri
Slavka Krautzeka 83/A
51000 Rijeka, Croatia
Phone: +385 (51) 770 447
Fax: +385 (51) 686 166
www.intechopen.com

InTech China
Unit 405, Office Block, Hotel Equatorial Shanghai
No.65, Yan An Road (West), Shanghai, 200040, China
中国上海市延安西路65号上海国际贵都大饭店办公楼405单元
Phone: +86-21-62489820
Fax: +86-21-62489821

© 2010 The Author(s). Licensee IntechOpen. This chapter is distributed under the terms of the Creative Commons Attribution-NonCommercial-ShareAlike-3.0 License, which permits use, distribution and reproduction for non-commercial purposes, provided the original is properly cited and derivative works building on this content are distributed under the same license.